DOI 10.1007/s11141-023-10202-w
Radiophysics and Quantum Electronics, Vol. 65, No. 3, August, 2022
(Russian Original Vol. 65, No. 3, March, 2022)

APPLICATION OF GYROTRONS FOR MOLECULAR GAS SPECTROSCOPY

**G. Yu. Golubyatnikov, M. A. Koshelev,*
A. I. Tsvetkov, A. P. Fokin, A. A. Ananichev,
M. Yu. Glyavin, and M. Yu. Tret'yakov**

UDC 535

We give a brief review of the results of using gyrotrons to study molecular spectra by means of a radioacoustic absorption detection (RAD) spectrometer. Examples of recording molecular spectral lines of sulfur dioxide (SO_2), carbon sulfide (OCS), and methane (CH_4) are presented. The achievement of a record-breaking sensitivity for the sub-terahertz frequency range in terms of the absorption coefficient is demonstrated when observing weak methane lines. The possibility of spectroscopy at harmonics of the gyrotron radiation with a frequency of up to 1 THz is shown. Spectroscopic estimates of the radiation power at the second and third harmonics with respect to the power at the fundamental frequency are given. The possibilities of using the methods of nonlinear spectroscopy, namely, two-photon spectroscopy, which extend the range of potential spectroscopic studies using intense gyrotron radiation, are demonstrated. The results of observations with a RAD spectrometer and a direct absorption spectrometer for the lines of two-photon rotational transitions of OCS and SO_2 molecules, which have well-studied spectra and a large dipole moment, are presented. Promising opportunities for using gyrotrons to solve fundamental and practical problems are discussed.

1. INTRODUCTION

This paper is a brief review of the results of using intense radiation of CRMs (cyclotron resonance masers) or gyrotrons for the purposes of molecular spectroscopy in the millimeter and submillimeter wavelength ranges, which were obtained at the IAP RAS over the past few years. This spectral range is interesting for gas spectroscopy due to its universal nature, i. e., the rotational spectra of almost all molecules fall exactly here, in contrast, e. g., to the vibration–rotational spectrum bands which can be widely scattered over the infrared range.

The history of discovery [1] and development of gyro devices at the IAP RAS is presented in many reviews, e. g., [2, 3]. The creation of gyrotrons operated in the submillimeter wavelength range [4] stimulated the desire to use this type of radiation sources for the study of molecular spectra. By the end of the 1960s, backward wave oscillators (BWOs, Istok, Fryazino) [5, 6] with a wide (up to an octave) frequency tuning in the submillimeter range and a power of several milliwatts were already produced in the USSR. Nevertheless, the significantly higher power of gyrotrons, despite their narrow frequency tuning within the cavity Q-factor, remained attractive to spectroscopists, who used the optoacoustic (OA) method. Such a technique was employed in a RAD spectromeer [7, 8]. The latter does not record a change in the radiation transmitted through the sample, as in conventional spectrometers, but the result of substance heating by radiation [9, 10]. Under the action of amplitude-modulated radiation, molecules are excited at the spectral transition

* koma@ipfran.ru

Institute of Applied Physics of the Russian Academy of Sciences, Nizhny Novgorod, Russia. Translated from Izvestiya Vysshikh Uchebnykh Zavedenii, Radiofizika, Vol. 65, No. 3, pp. 169–183, March 2022. Russian DOI: 10.52452/00213462_2022_65_03_169 Original article submitted April 27, 2022; accepted May 11, 2022.
0033-8443/22/6503-0157

frequency, and their collisional relaxation leads to gas heating and the appearance of modulation-frequency pressure pulsations detected by the deflection of a thin membrane, which is the sensing element of a condenser microphone.

In the early 1970s, this spectrometer with BWOs as radiation sources was widely employed at the IAP RAS [11–13] for the study of rotation–vibrational inversion spectra of molecules and precision measurements of the spectral line parameters [14]. The natural desire to combine RAD with gyrotron radiation to record weak spectral transitions is based on the OA signal growth with increasing power.

Such a demonstration experiment was conducted in 1974 at the IAP RAS [15]. A gyrotron operated at a frequency of 34 GHz with a radiation power of up to 1 kW was used. A molecule of formic acid HCOOH with a dipole moment of 0.1 D and, in particular, its transition $J_{K_a,K_c} = 6_{1.5} - 6_{1.6}$ was chosen for the study. The gyrotron radiation frequency did not have a smooth and reproducible tuning. The tuning was performed by mechanically varying the parameters of the slit resonator; therefore, the line width of the molecular transition had to be large enough, about 100 MHz. The required broadening was achieved due to the pressure of an extraneous gas, which reduced the absorption coefficient at the line maximum compared to the pure gas and ensured the absence of the molecular transition saturation effect. The response from the line depending on the radiation power was recorded by means of amplitude modulation. According to estimates, the absorption sensitivity achieved in the experiment was a record-breaking value for that time, about 10^{-11} cm^{-1} with a gyrotron power of 10^3 W. It is worth noting that this absorption detection method is frequency independent. Despite the successful demonstration, gyrotrons, due to their high cost, large sizes, and small radiation frequency tuning, could not compete with BWOs (a series of tubes continuously covered a frequency range of 30 GHz to 1.5 THz), which are compact and have a broadband smooth tuning of the radiation frequency by voltage. In addition, high-precision measurements of molecular spectra required the use of phase-locked loop (PLL) radiation systems based on a frequency and time standard signal, which were developed for BWOs [16, 17], but seemed inapplicable for gyrotrons (high voltage and high current for the control device).

The work of the University of Fukui (FIR FU, Japan) in the 2000s on the use of relatively low-power frequency-tunable gyrotrons for electron paramagnetic resonance (EPR) spectroscopy [18] and the application of a PLL gyrotron system with a diode electron gun [19] stimulated similar work at the IAP RAS. The analysis of spectroscopic problems requiring a high radiation power was performed [20] and test experiments on control and phase stabilization of the gyrotron frequency were carried out. For this purpose, a technological gyrotron with a triode configuration of the electron gun (the presence of a currentless anode for varying the pitch factor of the electron beam), which operated at a frequency of 12.3 GHz, was employed [21]. The high electrical capacity of both the control circuits of the gyrotron and the high-voltage power supply unit in the presence of high-frequency voltage pulsations of the cathode power supply unit precluded stable PLL operation. Nevertheless, a narrow, less than 10 kHz, gyrotron generation spectrum and the ability to control the radiation frequency by varying the frequency of the reference oscillator of the PLL system were demonstrated.

In the 2010s, gyrotrons with a power of about 100 W in the terahertz range [22, 23] were used for spectroscopy based on dynamic polarization of nuclei (DPN) and nuclear magnetic resonance (NMR). The related sensitivity improvement was almost two orders of magnitude. The importance of frequency and/or phase locked-loop operation and the possibility of fast frequency tuning of the gyrotron to improve the sensitivity of the DPN method is noted [24–26].

At the same time, an automated gyrotron facility with a cryomagnet and power supplies of increased stability was created at the IAP RAS [27, 28]. The appearance of gyrotrons operating in the subterahertz range made it possible to reconsider the possibility of using them in the interests of molecular spectroscopy [29]. The high intrinsic spectral stability of the gyrotron radiation (spectrum width of the order of 1 MHz) at a frequency of 263 GHz in the CW regime, enabled one to record a number of spectral transitions of the SO_2 molecule using RAD [30] with different radiation powers. The method of amplitude modulation of radiation was employed, and the frequency was varied by smooth tuning of the gyrotron cavity temperature.

The development and creation of a high-speed gyrotron anode voltage regulator at the IAP RAS [31] made it possible to fully implement the PLL using a reference microwave oscillator [32] and, as a result, precision control of the gyrotron radiation frequency [33]. The PLL system provided frequency/phase modulation (FM/PM) of gyrotron radiation [33], which is currently a necessary attribute of the practical use of radiation sources for metrological purposes.

A gyrotron stabilized in this way at a frequency of 263 GHz was employed to record spectral lines of SO_2, OCS, and CH_3OH molecules, as well as some weak lines of methane isotopologues (CH_4 and CH_3D), which have a small dipole moment, in order to estimate the limiting sensitivity by the absorption coefficient of the RAD spectrometer [33]. The high stability of the gyrotron radiation frequency in the PLL regime made it possible to apply the signal accumulation method and achieve a record-breaking sensitivity for the subterahertz range at $1.3 \cdot 10^{-11}\,\mathrm{cm}^{-1}$ with a radiation power of less than 20 W.

It has been shown that the available spectral range when working with a gyrotron can be extended by using the fundamental harmonic radiation contained in the gyrotron radiation [34–38]. This was demonstrated by the example of recording a number of rotational lines of SO_2, CH_3OH, and OCS molecules both at the fundamental (near 263 GHz) and at the second, third, and fourth harmonics of the gyrotron radiation frequency, i. e., up to 1 THz.

In order to demonstrate the possibility of further extending the range of spectroscopic problems that can be solved by means of high-power gyrotrons in the subterahertz range, we performed nonlinear two-photon absorption experiments, which require two radiation sources simultaneously. The frequency of one of them (e. g., the gyrotron) can be fixed, while the frequency of the second source (e. g., the BWO) can be scanned over the range. In our experiments, instead of the gyrotron, the radiation of two BWOs with a power of about 10 mW was used. The obtained results give a visual representation of how the type of the recorded spectrum will change when the BWO is replaced by a gyrotron.

Section 2 gives a brief description of the experimental setup. Section 3 is devoted to the results of measurement and analysis of spectral lines. Section 4 shows examples of application and analyzes the capabilities of nonlinear two-photon spectroscopy. In conclusion, examples of the potential use of the high radiation power characteristic of gyrotrons for solving fundamental and applied spectroscopy problems are given.

2. EXPERIMENTAL SETUP

A detailed description of the parameters of the gyrotron used as a source of continuous coherent radiation in a RAD spectrometer can be found in [27, 28]. The radiation spectral line width with a PLL system did not exceed 1 Hz [32]. Frequency stability was determined by the frequency and time standard (SRS FS740), based on a signal from the global navigation system, and was of the order of 10^{-13} and 10^{-11} for long- and short-term relative stability, respectively. The electronic frequency tuning range achieved by varying the intermediate frequency in a closed ring of the PLL was on the average 20 MHz, reaching 60 MHz with certain gyrotron parameters. A wider smooth tuning of the gyrotron frequency in the PLL regime was provided by varying the magnetic field and cathode voltage and due to controlled variation of the cavity temperature (4 MHz/°C). The achieved full range of gyrotron frequency tuning in PLL regime was 262.8–264.0 GHz with adjustable radiation power within 10–500 W.

The gyrotron radiation was directed to a matched load, and the gyrotron power was measured using a water calorimeter. Part of the radiation was directed into the measuring cell of the RAD spectrometer by means of a quasi-optical divider (a mica plate with a thickness of 20–40 μm, much shorter than the wavelength). The radiation intensity in the cell was estimated in two ways, namely, a) as the difference between calorimeter readings in the presence and absence of a divider in the path and b) by the width of the saturated spectral line using spectroscopic information about the magnitude of the matrix element of the dipole moment of the transition and the width of the unsaturated line. The values obtained by different methods were in good agreement with each other.

In a RAD spectrometer, the sensitivity does not depend on radiation frequency and allows absorbed

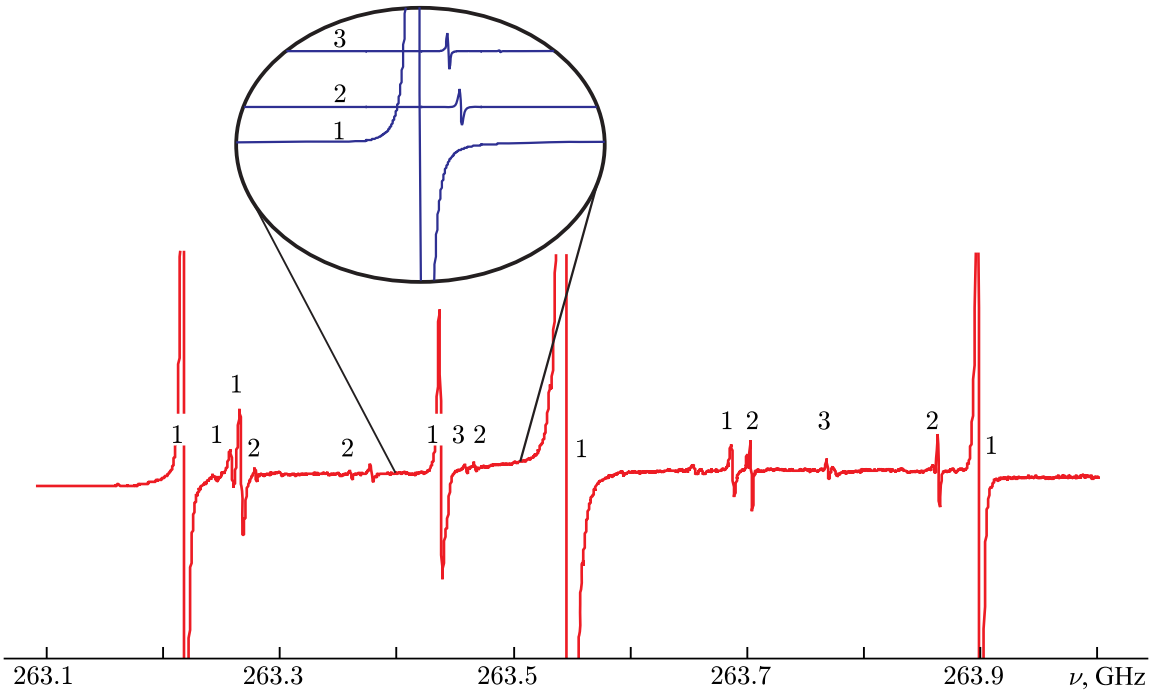

Fig. 1. A panoramic spectrum of SO_2 mixed with argon, recorded using a RAD spectrometer and a frequency-stabilized gyrotron. The number near the line corresponds to the harmonic number of the radiation frequency at which this line is observed. Fragments of the calculated spectrum of SO_2 on the fundamental, second, and third harmonics of radiation are shown in the inset.

power to be detected at a level of up to 10^{-10} W even with a small optical cell length ($L = 10$ cm) [11, 39, 40]. Most of the radiation that does not interact with the gas passes through the cell without any effect, i. e., no signal outside the absorption line takes place, which is the advantage of the method when high-power radiation is used. Within the absorption line, the output signal of the spectrometer is proportional to the power of the radiation absorbed by the gas in the cell, and the use of radiation sources with higher power increases the sensitivity of this spectrometer type.

The diameter and length of the absorbing cell of the RAD spectrometer used in the experiments were 2 and 20 cm, respectively. The acoustic signal was detected by a condenser microphone, the system for recording the capacitance variation of which is made in the form of a high-frequency balanced bridge circuit [41].

A block diagram of the RAD spectrometer with a gyrotron and a frequency stabilization system of the gyrotron radiation is given in [33, Fig. 1].

3. MEASUREMENTS AND SPECTRAL LINE ANALYSIS

For the first studies, we chose the SO_2 molecule, since its rotation–vibrational spectrum is well explored, and the frequencies and intensities of spectral transitions falling within the gyrotron generation range can be found in databases [42–44]. The details of this study are presented in [33].

In order to record low-intensity lines, the method of frequency modulation of the radiation, followed by demodulation of a signal from the OA receiver based on a synchronous detector, both at the first and second harmonics of the modulation frequency, was employed.

When analyzing the experimental spectrum of SO_2 shown in Fig. 1, it turned out that part of the observed lines is due to the absorption of radiation at a strictly doubled and tripled frequency of the gyrotron radiation, or at the second and third harmonics. The power of the harmonic radiation coming into the cell was estimated from known intensities of the observed spectral lines and was about 1 and 0.1% relative to

the power of the fundamental harmonic, respectively. The calculated spectra of SO_2 in the frequency ranges corresponding to the fundamental, second, and third radiation frequency harmonics, on the basis of which the experimental spectrum was analyzed, are presented in the inset to Fig. 1.

In order to analyze the gyrotron radiation and confirm the radiation harmonic generation, in addition to an accurate spectroscopic method based on the observation of known gas lines, quasi-optical high-pass filters (HPF), made in the form of perforated plates with many waveguide channels, the diameter of which corresponds to the cutoff frequency of a circular waveguide, were employed.

The filters used transmitted radiation with a frequency higher than the cutoff frequency 300 and 600 GHz. The result of applying an HPF with a cutoff frequency of 300 GHz to analyze the spectrum of SO_2 is shown in Fig. 2. The line at a frequency of 263.686 GHz disappears in the spectrum when using the mentioned filter, while the other two lines in the spectrum remain virtually unchanged, which is evidence for their higher-frequency nature. This is also indicated by the fact that the lines corresponding to the second harmonic are twice as wide on the record as the lines corresponding to the fundamental radiation frequency.

Figure 3 shows the result of observing the SO_2 line at a frequency of 1.0559 THz at the fourth harmonic of the fundamental gyrotron radiation frequency. In order to reduce the effect of radiation on the fundamental and second harmonics of the gyrotron frequency, an HPF with a cutoff frequency of 600 GHz was employed. The radiation power entering the cell at the frequency of the 4th harmonic was estimated from the known intensity of this line as 0.001% of the fundamental harmonic power.

Thus, the analysis of the experimental spectrum of a known gas obtained using a RAD spectrometer makes it possible to unambiguously determine the spectral composition of the radiation source used. In other words, a RAD spectrometer cell filled with a gas having a well-known and sufficiently dense spectrum can be used as a precision broadband spectrum analyzer of coherent radiation from powerful sources.

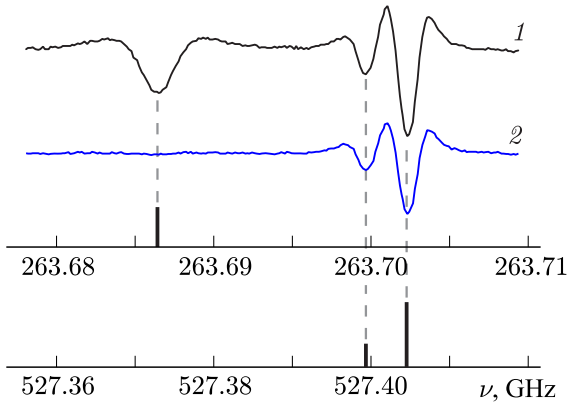

Fig. 2. The spectrum of SO_2 in a mixture with argon, obtained with and without HPF (curves *1* and *2*, respectively). Vertical lines indicate the positions of SO_2 transitions from the HITRAN database [44].

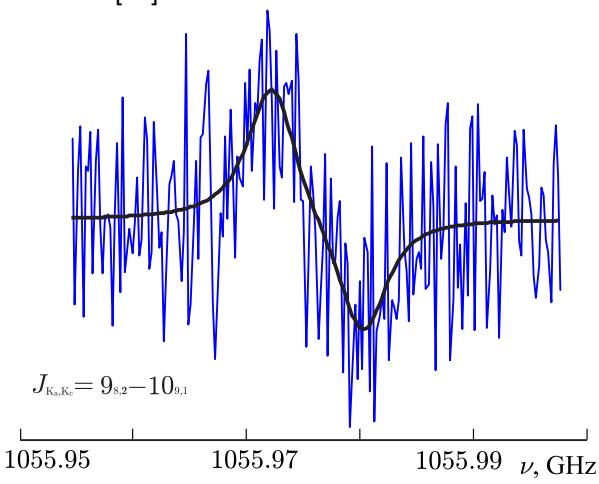

Fig. 3. The spectrum of the SO_2 mixture with argon in the range of the 1055976.3 MHz absorption line at the fourth harmonic of the gyrotron radiation. The solid line corresponds to a Voigt profile model optimized for the observed spectrum.

4. SATURATION EFFECTS AND SPECTROMETER SENSITIVITY

The main physical limitation on the power of the radiation sources used is the spectral transition saturation effect [45, 46], in which the level populations line up and, as a consequence, the absorption coefficient decreases and the line becomes broader. We observed a similar behavior in the experimental spectra of SO_2 obtained by the OA method using a frequency-stabilized gyrotron. This is demonstrated in Fig. 4. As the power is increased, the amplitudes of the lines decrease, and the lines themselves become broader and begin to disappear in experimental noise.

An increase in the signal from the line with increasing radiation power will be observed until the saturation of this transition. For typical OA spectroscopy pressures of the studied gas of the order of 1 Torr

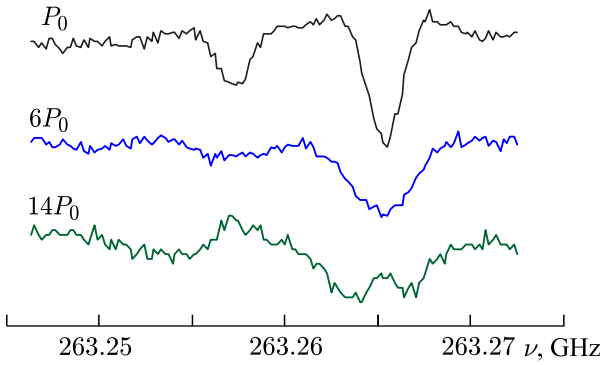

Fig. 4. Demonstration of the saturation effect of the lines of two molecular transitions at frequencies of 263.257 and 263.265 GHz with increasing pump power (indicated near the curves). A mixture of SO_2 with argon (partial pressures of 27 and 260 mTorr, respectively); $P_0 \sim 0.1$ W.

and a small matrix element of the dipole moment of transition of the molecule of the order of 0.1 D, saturation is observed even with a power flux of the order of 1 W/cm^2 [12]. The signal from the line is maximum at the radiation power $P^{\max} \propto n^2 S$ [12] and is determined only by the number of gas molecules interacting with the field (n is the particle concentration and S is the cross-sectional area of the electromagnetic beam interaction with the gas). Therefore, to avoid saturation of a homogeneously broadened line with increasing radiation power, it is necessary to reduce the power flux density (increase S) or increase the gas pressure (the linewidth is proportional to the particle concentration: $\Delta\nu \propto n$).

In order to estimate the spectrometer sensitivity by the absorption coefficient depending on the power, the ratio of the signal to the noise floor on the observed line of the SO_2 molecule at a frequency of 263151.53 MHz was employed (see Fig. 5). The minimum detectable absorption for the recording time of the spectrum of the order of 10 min and the radiation power of about 1 W corresponded to the absorption coefficient $\alpha^{\min} \approx 8 \cdot 10^{-10}$ cm^{-1}. For a spectrometer with the use of BWO radiation (a power of the order of 5 MW) this value did not exceed 10^{-8} cm^{-1} with a spectrum recording time of 100 min. This confirms that an

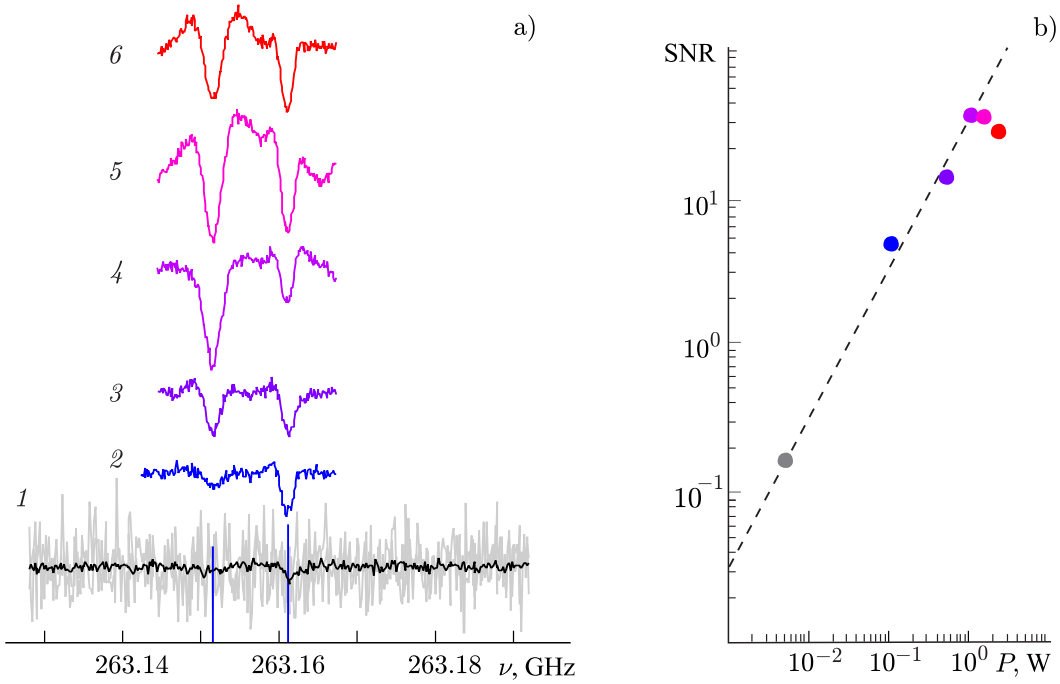

Fig. 5. Panel *a*. The spectrum of SO_2 molecules (mixed with argon in proportion 1:14) at a pressure of the order of 0.5 Torr. The lower spectrum was obtained using a BWO (a single record and averaging over 50 single records are shown in gray and black, respectively; the values corresponding to the gray curve are increased by $\sqrt{50}$ times) and the other spectra, using a frequency-stabilized gyrotron. Curves *1*, *2*, *3*, *4*, *5*, and *6* correspond to the radiation power $P = 0.005$, 0.1, 0.5, 1.0, 1.5, and 2.2 W. Panel *b*. Signal-to-noise ratio (SNR) for experimental records of the line at a frequency of 263.151 GHz (the position of the line in the spectrum and the position of the neighboring line, which is slightly more intense, are marked with vertical lines on the panel *a*) as functions of the radiation power P. The dashed line corresponds to a straight line passing through the origin of coordinates.

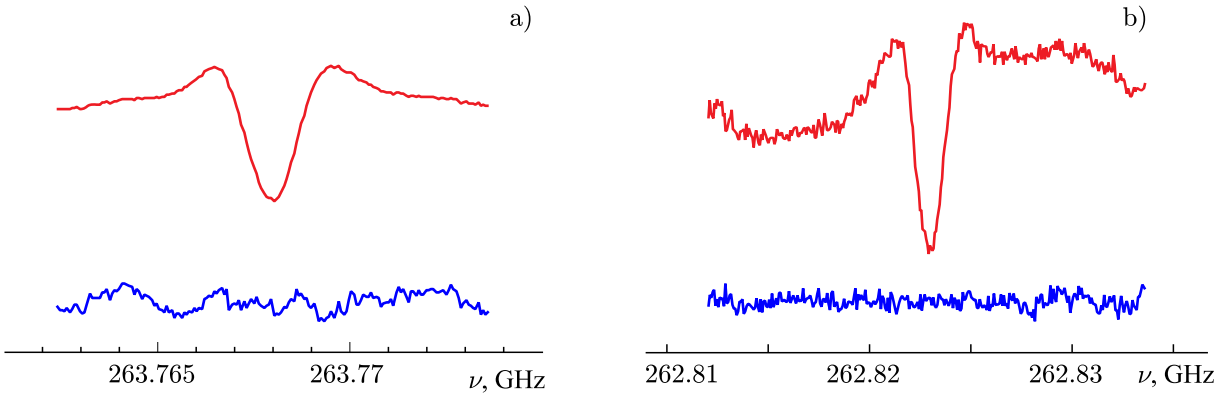

Fig. 6. Spectra of the molecules of CH_4 (*a*) and CH_3D (*b*) near transitions $J_K = 7_2 \leftarrow 6_4$ (state $\nu_4 + \nu_5$) and $8_2 \leftarrow 8_3$ (E-type, state ν_5), recorded using a RAD spectrometer (high-density polyethylene cell windows) and a gyrotron when averaging 104 (*a*) and 40 (*b*) single spectrum records. The residuals of approximation of experimental spectra by the model profile are shown below (on panel *a* the residual is increased by 5 times). The absorption coefficient at the line maximum is $1 \cdot 10^{-9}\,\mathrm{cm}^{-1}$ (*a*) and $6 \cdot 10^{-10}\,\mathrm{cm}^{-1}$ (*b*); SNR ~ 80 (*a*) and 30 (*b*).

increase in the power of the probing radiation leads to a proportional increase in the sensitivity of the spectrometer to the limit related to the molecular transition saturation (see Fig. 5).

When observing the spectral lines of molecules of methane CH_4 and its isotopologue CH_3D, the saturation effect should be manifested at significantly higher levels of radiation intensity (more than 1 kW/cm^2), since the corresponding transitions have a small dipole moment (less than 0.01 D) caused by centrifugal distortion of the symmetric structure of the rotating molecule and isotope substitution of one of the protons. Observation of the lines of these molecules (see Fig. 6) made it possible to achieve a sensitivity of the order of $10^{-11}\,\mathrm{cm}^{-1}$ at a radiation power of about 15 W [33].

The use of a high radiation power leads to the fact that the presence of even a small absorption in the input/output window of the gas cell leads to the heating of the molecules.

The temperature of the RAD cell copper body, which served as a natural heat sink, was about 40–60 °C at a radiation power of about 15 W. This did not allow using a higher power. In order to avoid overheating of the windows of the gas cell for RAD, windows made of polycrystalline diamond produced using a vapor deposition technology were employed. The tangent of the dielectric loss angle of such windows in the frequency range 100–350 GHz measured by the cavity method is of the order of $(0.3\text{–}1.0) \cdot 10^{-5}$ [47, 48].

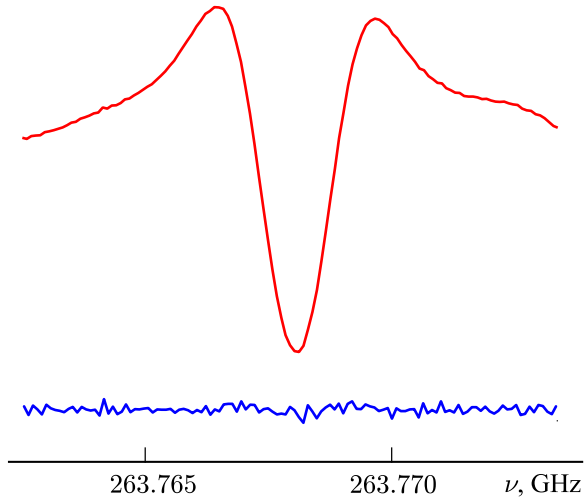

Fig. 7. A record of the CH_4 molecule line (transition $J_K = 7_2 \leftarrow 6_4$, $\nu_4 + \nu_5$) averaged over 200 scans using a RAD spectrometer (with diamond windows) and gyrotron radiation with a power of about 60 W. The residual of approximation of the experimental spectrum by the model profile, increased by 5 times, is shown below. Absorption coefficient at the line maximum is $1 \cdot 10^{-9}\,\mathrm{cm}^{-1}$; SNR ~ 330.

In addition to increasing the radiation power, digital signal accumulation, which is possible due to the use of the PLL system, was employed to demonstrate the maximum achievable sensitivity in this version of a RAD spectrometer. Two hundred records of the rotational spectrum line of the CH_4 molecule were averaged at a frequency of 263767.94 MHz with a radiation power of about 60 W (see Fig. 7). The absorption-

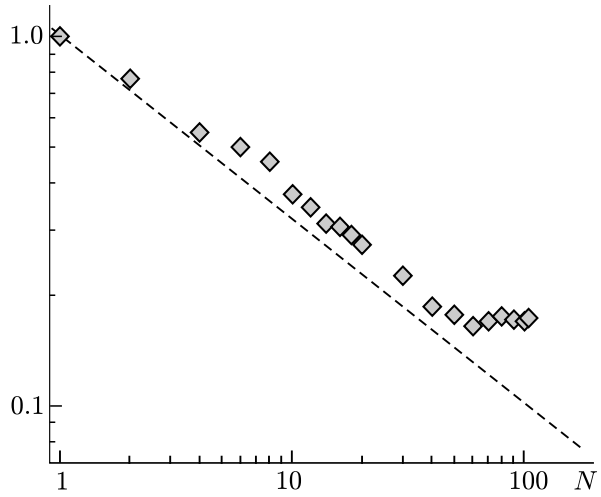

Fig. 8. Reduction of the noise level (standard deviation of the experimental points from the model function, normalized to the value at $N = 1$) when recording the line of the CH_4 molecule at a frequency of 263767.94 MHz with an increase in the number N of averaged spectra. The dashed line shows the function $N^{-0.5}$ corresponding to the averaging of noise in a stationary process.

coefficient sensitivity of the spectrometer was estimated from the known transition intensity and the SNR calculated from the averaged experimental spectrum and was of the order of $3 \cdot 10^{-12}\,\mathrm{cm}^{-1}$. This value is approximately 4 times higher than the sensitivity we obtained earlier [33] and is a record-breaking one for the subterahertz frequency range.

The drift of the gyrotron power and its dependence on frequency lead to unsteady heating of the gas cell, which imposes restrictions on increasing sensitivity with the further increase in the number of averagings (see Fig. 8). The most probable influencing factors are both power variations related to the operation of the automatic frequency control system and the drift of the magnitude of the spurious acoustic signal related to the heating of the cell elements and secondary gas heating. Stabilization of the gyrotron radiation power is highly desirable, but is technically difficult to implement. Another way to solve this problem is to use fast scanning of the gyrotron frequency. The rate of scanning should be such that the line contour is recorded within a time much shorter than the characteristic time of non-stationary processes that lead to both changes in the radiation power and variations in the spurious signal amplitude. This operation mode was implemented by us using a cavity spectrometer [49].

Note that when using gyrotrons operated in a pulsed mode, the absorption signal in the sample under study can be separated from the secondary spurious signal related to non-radiative heating of the cell gas by using a temporal signal resolution method [50].

5. NONLINEAR SPECTROSCOPY OF TWO-PHOTON TRANSITIONS

The high radiation power of the gyrotron enables one to use nonlinear methods for spectroscopy of molecular gas mixtures, namely, two-photon (two-quantum) absorption [51, 52]. The two-photon absorption cross section is many orders of magnitude smaller than the single-photon absorbtion cross section, which removes the spectroscopic limitation related to the saturation effect. When using high-power lasers (a power flux of up to $10^9\,\mathrm{W/cm}^2$ or more), two-photon absorption is easily observed in experiment; therefore, two-photon spectroscopy has become widespread [52].

It was shown in [53] that the power flux at a level of 1 $\mathrm{W/cm}^2$ of such a radiation source as an orotron at a wavelength of 2 mm makes it possible to observe two-photon rotational transitions of OCS and fluoroform molecules (CHF_3).

The system of levels and the scheme of two-photon molecular transitions is shown in Fig. 9. The probability of a two-photon transition $0 \to\to 2$ from the level 0 to the level 2 for bound transitions $0 \to 1$ and $1 \to 2$, which have a common level 1, is proportional to the matrix element squared (non-degenerate case)

$$\langle \mu E \rangle_{0\to\to 2} = \langle \mu_{01} E_1 \rangle \, \langle \mu_{12} E_2 \rangle / (2\hbar \Delta\omega), \tag{1}$$

where $\Delta\omega$ corresponds to the difference between the radiation frequency and the transition frequency, $\hbar$ is the Planck constant, μ_{01} and μ_{12} are the matrix elements of the transitions $0 \to 1$ and $1 \to 2$ with frequencies ω_{01} and ω_{12}, and E_1 and E_2 are the the electric fields of radiation at frequencies ω_1 and ω_2, respectively, i. e., $\Delta\omega = \omega_1 - \omega_{01} = \omega_{12} - \omega_2$, while $\omega_1 + \omega_2 = \omega_{01} + \omega_{12}$. Note that when the radiation frequencies and the transitions $\Delta\omega = 0$ coincide, a double resonance method, which is conventional for spectroscopy and permits

changing the level population and increasing the sensitivity for the corresponding transition, is employed (see, e. g., [54]).

In order to demonstrate the possibility of using a two-photon transition method and to estimate its sensitivity, experiments with a RAD spectrometer and a video spectrometer (cell length 2 m) were performed [55]. Two OV-71 type BWOs (a frequency of 75–130 GHz) were used as radiation sources in a configuration with counterpropagating waves of orthogonal polarizations. Wire polarizers were employed to reduce the mutual effect on the BWO radiation generation. The radiation from one source was fixed in frequency, while the radiation from the other was frequency-modulated and tuned in frequency to record the spectrum. The radiation power of both BWOs did not exceed 10 mW.

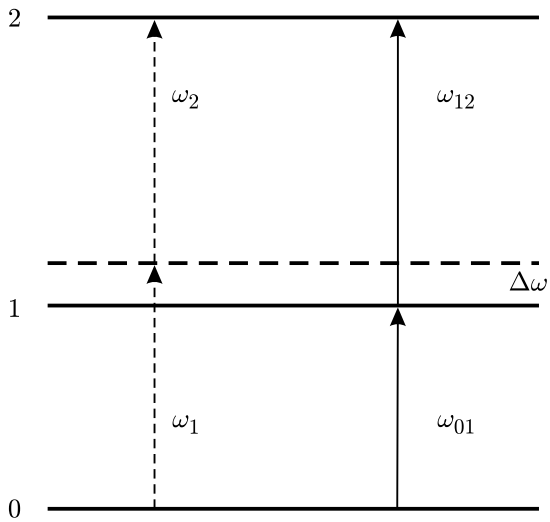

Fig. 9. Scheme of allowed molecular transitions. Solid thick horizontal lines show the molecule energy levels 0, 1, and 2. The dashed line shows the virtual level, thin solid arrows show regular single-photon transitions, and dashed arrows show two-photon transitions.

In order to record the absorption spectrum, rotational transitions of OCS and SO_2 molecules with a high dipole moment (0.7 D and 1.6 D, respectively), the lines of which are well studied, were chosen. According to Eq. (1), the intensity of the two-photon transition decreases in inverse proportion to $(\Delta\omega)^2$; therefore, the detuning of the radiation frequency from the spectral transition frequency was chosen relatively small $\Delta\omega/(2\pi) < 10$ MHz. In this case, two lines, namely, a single-photon transition line (ω_{01} or ω_{12}) and a two-photon resonance line are observed at once.

For studies of OCS molecules, the transitions $8 \leftarrow 7$ ($\omega_{01}/(2\pi) = 97301.2$ MHz) and $9 \leftarrow 8$ ($\omega_{12}/(2\pi) = 109463.06$ bound by a common rotational level $J = 8$ were used and the transition $9 \leftarrow\leftarrow 7$, which could be observed at the frequency of two-photon resonance ($\omega_{02} = \omega_{01} \pm \Delta\omega$ or $\omega_{02} = \omega_{12} \pm \Delta\omega$), were employed. In SO_2, transitions $3_{1,3} \leftarrow 2_{0,2}$ ($\omega_{01}/(2\pi) = 104029.4$ MHz) and $2_{2,0} \leftarrow 3_{1,3}$ ($\omega_{12}/(2\pi) = 100878.1$ MHz) bound by a common rotational level $J_{K_a,K_c} = 3_{1,3}$ were chosen. Two-photon resonance was observed for the transition $2_{2,0} \leftarrow\leftarrow 2_{0,2}$.

A fragment of the spectrum in the region of the transition line $8 \leftarrow 7$ at an OCS pressure of 0.1 Torr in the cell and the two-photon resonance line as a function of $\Delta\omega$ on the spectrometer with RAD are shown in Fig. 10. It can be seen that the amplitude of the two-photon resonance line decreases rapidly as the detuning $\Delta\omega$ is increased.

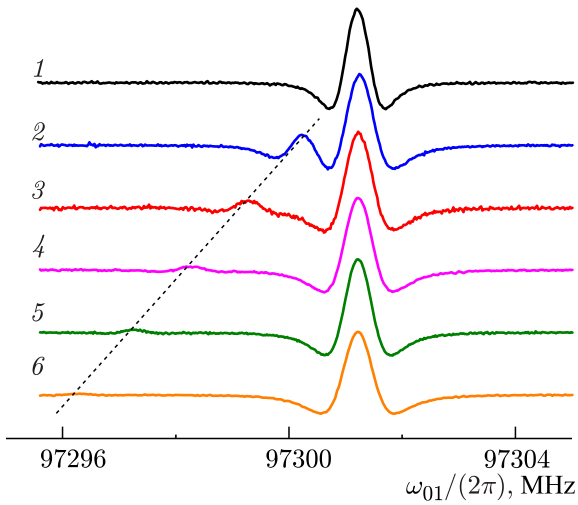

Fig. 10. Fragments of the OCS spectrum recorded using a RAD spectrometer with one radiation source (curve *1*; rotational transition $8 \leftarrow 7$ at the frequency $\omega_{01}/(2\pi) = 97301.2$ MHz); with simultaneous operation of two radiation sources (the frequency $\omega_{02}/(2\pi)$ is fixed): $\omega_{02}/(2\pi) = 109464.0$ MHz (*2*), $\omega_{02}/(2\pi) = 109465.0$ MHz (*3*), $\omega_{02}/(2\pi) = 109466.0$ MHz (*4*), $\omega_{02}/(2\pi) = 109467.0$ MHz (*5*), $\omega_{02}/(2\pi) = 109468.0$ MHz (*6*), and SNR = 10. The frequency of the bound transition $9 \leftarrow 8$ is $\omega_{02}/(2\pi) = 109463.06$ MHz. The pressure in the cell is 0.1 Torr. The dashed line connects the centers of the two-photon transition lines $9 \leftarrow\leftarrow 7$.

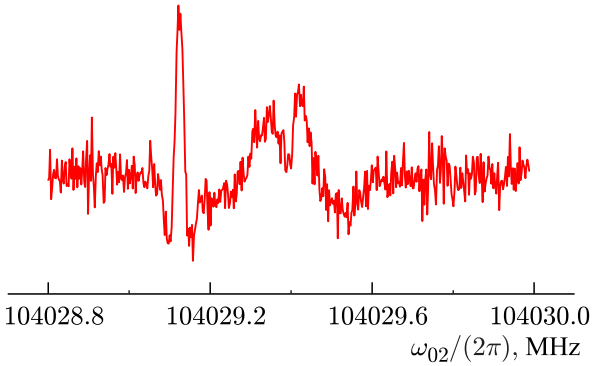

Fig. 11. The spectrum of SO_2 in the region of the two-photon resonance line, recorded using a video spectrometer. The frequency of the first quantum is $\omega_{01}/(2\pi) = 100878.4$ MHz. The SO_2 pressure in the cell is 0.7 mTorr and the cell length is 2 m.

At low pressures (less than 1 mTorr), a Lamb dip and a narrowed two-photon resonance line, which is free from Doppler broadening, were observed at the top of the Doppler-broadened line of one of the bound transitions ($J_{K_a,K_c} = 3_{1,3} \leftarrow 2_{0,2}$ at a frequency of 104029.4MHz; see Fig. 11).

With the increase in the radiation power of one of the sources (e. g., when the BWO, the frequency of which is fixed, is replaced by a gyrotron), the probability of a two-photon transition and, consequently, the sensitivity of detecting the corresponding line using a RAD spectrometer will increase proportionally. The saturation effect does not occur, since the gyrotron frequency does not coincide with the transition frequency. For example, when radiation with a power of the order of 100 W (which is a factor of 10^4 greater than the BWO power) is used and the detuning $\Delta\omega/(2\pi) = 10$ MHz, the sensitivity (i. e., SNR) will increase by more than 1000 times. Since the line intensity of a two-photon transition decreases as $(\Delta\omega)^{-2}$, the frequency detuning at which the line will be observed with the same SNR will increase only by 100 times, i. e., from 10 MHz to 1 GHz.

When using a single radiation source in the experiment (as, e. g., in [53]), the frequency at which the two-photon resonance will be observed is equal to the average frequency of the bound transitions $\omega_1 = (\omega_{01}+\omega_{12})/2$. The frequency scanning range corresponds to twice the frequency tuning range of the gyrotron. Note that the two-quantum transition line cannot be observed at the second harmonic of radiation (which, as was shown above, is present in the gyrotron spectrum) due to non-compliance with the conservation of angular momentum in the molecule–quantum system.

Thus, the simultaneous use of two radiation sources, namely, a gyrotron with a fixed radiation frequency and a low-power source with a wide frequency tuning, e. g., BWO, makes it possible to

1) significantly increase the number of lines accessible for observation (the gyrotron generation band is determined by the cavity Q-factor and typically does not exceed $\Delta f/f \sim 10^{-3}$),

2) improve the frequency resolution in the counterpropagating-beam configuration (two-photon spectroscopy, free from Doppler broadening), and

3) increase sensitivity when recording weak lines or minor impurities with a large dipole moment without the spectral transition saturation effect.

6. CONCLUSIONS

It is shown that low-intensity molecular spectral lines can be recorded by the radioacoustic method with an absorption-coefficient sensitivity of the order of 10^{-11} cm^{-1} within a line recording time of 1–10 min. The high sensitivity was achieved due to the use of a gyrotron, the radiation power of which in the RAD cell did not exceed several tens of watts in these experiments, which is several orders of magnitude higher than the radiation power of the millimeter and submillimeter wave sources that are conventional for spectroscopy.

In terms of the development of the RAD method with powerful radiation sources, it seems promising to further improve the sensitivity by increasing the rate of scanning the radiation frequency to ensure that the line recording is faster than the characteristic time of the radiation power variation. This will enable us to move further towards increasing the power of the probing radiation and, consequently, detecting even weaker molecular lines corresponding to transitions with very small matrix elements of the dipole moment. As an example, we should mention the paramagnetic molecule transitions occurring due to the magnetic dipole moment, which is typically equal to about one Bohr magneton. This is equivalent to an electric dipole moment of about 0.01 D when the molecules interact with the radiation. Other examples of interest

for fundamental spectroscopy are studies of quadrupole transitions of nonpolar molecules forbidden in the electric-dipole approximation [56] or, e. g., measurement of the positronium fine structure [57]. Strictly forbidden transitions between spin isomers of molecules, i. e., transitions between para- and orthostates are even more interesting [58, 59]. Thus, in [60], an estimate, from which it follows that the presence of radiation sources in the millimeter wavelength range with a power flux of more than 0.1 W/cm^2 would make it possible to obtain a detectable change in the spin isomer ratio in $^{13}CH_3F$, was made.

Nonlinear two-photon spectroscopy methods can significantly increase the number of lines available for observation and increase sensitivity when recording weak lines or minor impurities with a large dipole transition moment without the spectral transition saturation effect.

The analysis of the gyrotron radiation spectrum carried out in this paper demonstrates a unique opportunity for using the RAD method to determine the exact frequency and power characteristics of radiation sources.

The work was supported by the Ministry of Science and Higher Education of the Russian Federation (state assignment No. 0030–2021–0016).

REFERENCES

1. A. V. Gaponov, M. I. Petelin, and V. K. Yulpatov, *Radiophys. Quantum Electron.*, **10**, Nos. 9–10, 794–813 (1967). https://doi.org/10.1007/BF01031607
2. V. A. Flyagin and G. S. Nusinovich, *Proc. IEEE*, **76**, No. 6, 644–656 (1988). https://doi.org/10.1109/5.4454
3. A. L. Goldenberg and A. G. Litvak, *Phys. Plasmas*, **2**, No. 6, 2562–2572 (1995). https://doi.org/10.1063/1.871218
4. A. A. Andronov, V. A. Flyagin, A. V. Gaponov, et al., *Infrared Phys.*, **18**, No. 6, 385–393 (1978). https://doi.org/10.1016/0020-0891(78)90045-3
5. M. B. Golant, R. L. Vilenkin, E. A. Zyulina, et al., *Prib. Tekhn. Éksper.*, No. 4, 136 (1965).
6. M. B. Golant, Z. T. Alekseenko, Z. S. Korotkova, et al., *Prib. Tekhn. Éksper.*, No. 3, 231–232 (1969).
7. L. B. Kreuzer, *J. Appl. Phys.*, **42**, No. 7, 2934–2943 (1971). https://doi.org/10.1063/1.1660651
8. V. P. Zharov and V. S. Letokhov, *Laser Opto–Acoustic Spectroscopy* [in Russian], Nauka, Moscow (1984).
9. A. F. Krupnov, L. I. Gershtein, V. G. Shustrov, and S. P. Belov, *Radiophys. Quantum Electron.*, **13**, No. 9, 1080–1082 (1970). https://doi.org/10.1007/BF01032778
10. A. V. Burenin, *Radiophys. Quantum Electron.*, **17**, No. 9, 984–994 (1974). https://doi.org/10.1007/BF01036889
11. A. F. Krupnov and A. V. Burenin, in: K. Narahari Rao, ed., *Molecular Spectroscopy: Modern Research, Vol. 2*, Academic Press, New York (1976), pp. 93–126.
12. A. F. Krupnov, in: G. W. Chantry, ed., *Modern Aspects of Microwave Spectroscopy*, Academic Press, London (1979), pp. 217–256.
13. https://mwl.ipfran.ru/
14. A. F. Krupnov, M. Yu. Tretyakov, S. P. Belov, et al., *J. Mol. Spectrosc.*, **280**, 110–118 (2012). https://doi.org/10.1016/j.jms.2012.06.010
15. I. I. Antakov, S. P. Belov, L. I. Gershtein, et al., *JETP Lett.*, **19**, No. 10, 329–330 (1974).
16. A. F. Krupnov, *Radiophys. Quantum Electron.*, **41**, No. 11, 923–934 (1998). https://doi.org/10.1007/BF02676461

17. A. F. Krupnov, *Int. J. Infrared Millim. Waves*, **22**, No. 1, 1–18 (2001). https://doi.org/10.1023/A:1010744901186

18. S. Mitsudo, T. Higuchi, K. Kanazawa, et al., *J. Phys Soc. Jpn. Suppl. B*, **72**, 172–176 (2003). https://doi.org/10.1143/JPSJS.72SB.172

19. T. Idehara, S. Mitsudo, and I. Ogawa, *IEEE Trans. Plasma Sci.*, **32**, No. 3, 910–916 (2004). https://doi.org/10.1109/TPS.2004.827599

20. G. Yu. Golubiatnikov, in: J. L. Hirshfield and M. I. Petelin, eds., *NATO Science Series II. Mathematics Physics and Chemistry, Vol. 203*, Springer, Dordrecht (2005), pp. 297–304. https://doi.org/10.1007/1-4020-3638-8_22

21. G. Yu. Golubyatnikov, A. F. Krupnov, L. V. Lubyako, et al., *Tech. Phys. Lett.*, **32**, No. 8, 650–652 (2006). https://doi.org/10.1134/S1063785006080037

22. M. Rosay, L. Tometich, S. Pawsey, et al., *Phys. Chem. Phys.*, **12**, No. 22, 5850–5860 (2010). https://doi.org/10.1039/c003685b

23. E. A. Nanni, A. B. Barnes, R. G. Griffin, and R. J. Temkin, *IEEE Trans. Terahertz Sci. Technol.*, **1**, No. 1, 145–163 (2011). https://doi.org/10.1109/TTHZ.2011.2159546

24. T. Idehara, E. M. Khutoryan, Y. Tatematsu, et al., *J. Infrared Millim. Terahertz Waves*, **36**, 819–829 (2015). https://doi.org/10.1007/s10762-015-0176-2

25. F. J. Scott, E. P. Saliba, B. J. Albert, et al., *J. Magn. Reson.*, **289**, 45–54 (2018). https://doi.org/10.1016/j.jmr.2018.02.010

26. C. Gao, N. Alaniva, E. P. Saliba, et al., *J. Magn. Reson.*, **308**, 106586 (2019). https://doi.org/10.1016/j.jmr.2019.106586

27. M. Yu. Glyavin, M. V. Morozkin, A. I. Tsvetkov, et al., *Radiophys. Quantum Electron.*, **58**, No. 9, 639–648 (2016). https://doi.org/10.1007/s11141-016-9636-3

28. M. Yu. Glyavin, A. V. Chirkov, G. G. Denisov, et al., *Rev. Sci. Instr.*, **86**, No. 5, 054705 (2015). https://doi.org/10.1063/1.4921322

29. M. Yu. Glyavin, G. G. Denisov, V. E. Zapevalov, et al., *Phys. Usp.*, **59**, No. 6, 595–604 (2016). https://doi.org/10.3367/UFNe.2016.02.037801

30. M. A. Koshelev, A. I. Tsvetkov, M. V. Morozkin, et al., *J. Molec. Spectrosc.*, **331**, 9–6 (2017). https://doi.org/10.1016/j.jms.2016.10.014

31. B. Z. Movshevich, A. I. Tsvetkov, M. Yu. Glyavin, and A. P. Fokin, *Instrum. Exp. Tech.*, **63**, No. 6, 830–834 (2020). https://doi.org/10.1134/S002044122006010X

32. A. P. Fokin, M. Glyavin, G. Golubiatnikov, et al., *Sci. Rep.*, **8**, 4317 (2018). https://doi.org/10.1038/s41598-018-22772-1

33. G. Yu. Golubiatnikov, M. A. Koshelev, A. I. Tsvetkov, et al., *IEEE Trans. Terahertz Sci. Technol.*, **10**, No. 5, 502–512 (2020). https://doi.org/10.1109/TTHZ.2020.2984459

34. B. G. Danly, W. J. Mulligan, R. J. Temkin, and T. C. L. G. Sollner, *Appl. Phys. Lett.*, **46**, 728–730 (1985). https://doi.org/10.1063/1.95489

35. S. Alberti, M. Pedrozzi, M. Q. Tran, et al., *Phys. Fluids B. Plasma Phys.*, **2**, No. 11, 2544–2546 (1990). https://doi.org/10.1063/1.859377

36. G. S. Nusinovich and A. B. Pavel'ev, *Radiotekh. Élektron.*, **32**, No. 6, 1274–1280 (1987).

37. N. A. Zavol'skii, G. S. Nusinovich, and A. B. Pavel'ev, *Radiophys. Quantum Electron.*, **31**, No. 3, 269–275 (1988). https://doi.org/10.1007/BF01080391361–368

38. M. Yu. Glyavin, A. P. Gashturi, I. V. Zotova, et al., *45th Intern. Conf. Infrared, Millimeter, and Terahertz Waves, November 8–13, 2020*, Buffalo, USA. https://doi.org/10.1109/IRMMW-THz46771.2020.9370405

39. A. F. Krupnov and A. V. Burenin, *Radiophys. Quantum Electron.*, **22**, No. 3, 209–215 (1979). https://doi.org/10.1007/BF01034905

40. A. V. Burenin and A. F. Krupnov, *Radiophys. Quantum Electron.*, **17**, No. 8, 946–948 (1974). https://doi.org/10.1007/BF01037097

41. L. I. Gershtein, *Radiophys. Quantum Electron.*, **20**, No. 2, 148–154 (1977). https://doi.org/10.1007/BF01034201

42. https://spec.jpl.nasa.gov/ftp/pub/catalog/catform.html

43. https://cdms.astro.uni-koeln.de/

44. I. E. Gordon, L. S. Rothman, R. J. Hargreaves, et al., *J. Quant. Spectrosc. Radiative Transfer*, **277**, 107949 (2022). https://doi.org/10.1016/j.jqsrt.2021.107949

45. W. Demtroeder, *Laser Spectroscopy. Basic Concepts and Instrumentation*, Springer, Berlin (2003).

46. C. H. Townes and A. L. Schawlow, *Microwave Spectroscopy*, Mc Graw-Hill, New York (1955).

47. E. V. Koposova, S. E. Myasnikova, V. V. Parshin, and S. N. Vlasov, *Diam. Relat. Mater.*, **11**, 1485–1490 (2002). https://doi.org/10.1016/S0925-9635(02)00051-1

48. V. V. Parshin, B. M. Garin, S. E. Myasnikova, and A. V. Orlenekov, *Radiophys. Quantum Electron.*, **47**, No. 12, 974–981 (2004). https://doi.org/10.1007/s11141-005-0039-0

49. A. F. Krupnov, M. Yu. Tretyakov, V. V. Parshin, et al., *J. Mol. Spectrosc.*, **202**, 107–115 (2000). https://doi.org/10.1006/jmsp.2000.8104

50. A. B. Tikhomirov and B. A.Tikhomirov, *Opt. Atm. Okeana*, **28**, No. 12, 1112–1121 (2015). https://doi.org/10.15372/AOO20151209

51. T. Oka, in: R. G. Brewer and A. Mooradian, eds., *Laser Spectroscopy*, Plenum Press, New York (1974), pp. 413–432.

52. V. S. Letokhov and V. P. Chebotaev, *Ultra-High Resolution Nonlinear Laser Spectroscopy* [in Russian], Nauka, Moscow (1990).

53. L. A. Surin, B. S. Dumesh, F. S. Rusin, et al., *Phys. Rev. Lett.*, **86**, No. 10, 2002–2005 (2001). https://doi.org/10.1103/PhysRevLett.86.2002

54. J. I. Steinfeld and P. L. Houston, in: J. I. Steinfeld, ed., *Laser and Coherence Spectroscopy*, Springer, Boston (1978), pp. 1–123. https://doi.org/10.1007/978-1-4684-2352-5_1

55. G. Yu. Golubiatnikov, S. P. Belov, and A. V. Lapinov, *Radiophys. Quantum Electron.*, **58**, No. 8, 622–631 (2015). https://doi.org/10.1007/s11141-016-9634-5

56. A. V. Burenin and A. F. Krupnov, *Sov. Phys. JETP*, **40**, No. 2, 252–253 (1975).

57. O. Dumbrajs and T. Idehara, *J. Infrared Millim. Terahertz Waves*, **31**, No. 11, 1265–1270 (2010). https://doi.org/10.1007/s10762-010-9709-x

58. J. T. Hougen and T. Oka, *Science*, **310**, 1913–1914 (2005). https://doi.org/10.1126/SCIENCE.1122110

59. H. Kanamori, Z. T. Dehghani, A. Mizoguchi, and Y. Endo, *Phys. Rev. Lett.*, **119**, 173401 (2017). https://doi.org/10.1103/PhysRevLett.119.173401

60. O. I. Permyakova, E. Ilisca, and P. L. Chapovsky, *Phys. Rev. A*, **67**, 033406 (2003). https://doi.org/10.1103/PhysRevA.67.033406